Volume 20 | Number 47 | 21 December 2018 | Pages 7613–7740

CrystEngComm

rsc.li/crystengcomm

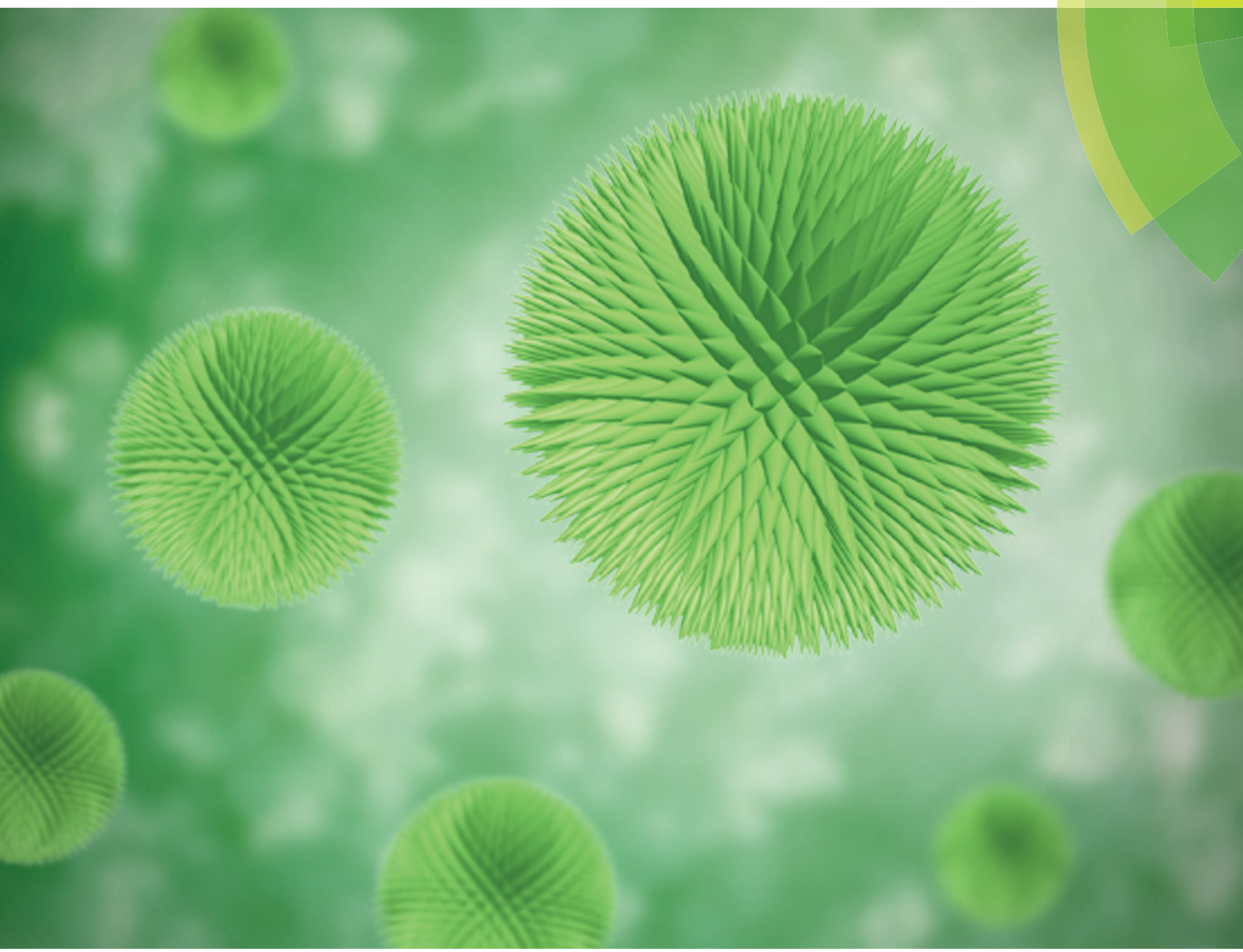

ROYAL SOCIETY OF CHEMISTRY

COMMUNICATION

Jing Wei *et al.*

Synthesis of spiny metal–phenolic coordination crystals as a sensing platform for sequence-specific detection of nucleic acids

CrystEngComm

COMMUNICATION

View Article Online
View Journal | View Issue

Cite this: *CrystEngComm*, 2018, **20**, 7626

Received 12th September 2018,
Accepted 16th October 2018

DOI: 10.1039/c8ce01555d

rsc.li/crystengcomm

Synthesis of spiny metal–phenolic coordination crystals as a sensing platform for sequence-specific detection of nucleic acids†

Hengbo Huang, Jing Qin, Gen Wang, Zehua Guo, Xu Yu, Yongxi Zhao and Jing Wei *

Spiny metal–phenolic coordination crystals are synthesized using a nontoxic plant polyphenol as a ligand. Due to the abundance of metal species and sp^2-hybridized carbon atoms on their spiny surface, such coordination crystals can adsorb DNA probes and quench the fluorescence, resulting in a high efficiency for nucleic acid assay.

Metal–organic coordination polymers (such as metal–organic frameworks), assembled from metal species and organic ligands, have attracted increasing attention due to their high surface area, tailorable compositions and various applications in adsorption, separation, catalysis, sensors and biomedicine.[1] Metal–phenolic coordination polymers (MPCPs), as a subclass of metal–organic coordination polymers, are usually synthesized using a plant polyphenol as an organic ligand based on the coordination interactions between catechol groups and metal species.[2] Plant polyphenols, as naturally abundant compounds, are widely present in fruits, vegetables and other plants. Most importantly, plant polyphenols can be directly extracted on an industrial scale.[3] Due to the low cost, nontoxicity, sustainability and good adhesive properties of the organic ligand, MPCPs have been widely used for surface engineering, drug delivery, imaging, catalysis and sensors.[4] The synthesis of MPCPs with tunable compositions and architectures can further tailor the physiochemical properties and improve the performance for various applications. Till now, MPCP capsules and colloidal spheres have been synthesized. However, the synthesis of MPCPs with intricate architectures and crystalline frameworks is still a great challenge.

Recently, metal–organic coordination polymers have been regarded as a versatile fluorescent probe for the detection of various biomolecules, and can potentially be used in clinical diagnosis.[5] For example, coordination polymers can adsorb fluorescently labeled probe DNA and the fluorescence of the probe can be quenched. However, when the target DNA is present, it can trigger a hybridization reaction with the probe DNA. The formation of double-stranded structures can weaken the interactions between the materials and DNA. Consequently, the double-stranded structure of the DNA will detach from the coordination polymers, leading to the recovery of fluorescence. Based on this feature, the restoration of fluorescence can be applied to the quantitative analysis of the target DNA.

The particle size, surface groups and charges, and metal species of coordination polymers can affect their interactions with dye-labeled biomolecule probes.[5i] As a result, coordination polymers with different morphologies, compositions and surface modifications have been synthesized and used to realize the detection of the target DNA with high sensitivity and selectivity.[5h] Most coordination polymers used for the detection of nucleic acids have nanoporous structures with small pore size (<2 nm), which limits the encapsulation of DNA molecules. As a result, probe DNA molecules are usually adsorbed on the surface of coordination polymers. Such coordination polymers usually have crystalline frameworks with a smooth surface, which can only provide limited interaction sites for DNA molecules. The design of coordination polymers with a rough surface would be beneficial for loading DNA probes. Inspired by the structure of a virus with a spiny surface, particles with a virus-like surface would promote the interactions with guest molecules.[6] It is believed that coordination polymers with a spiny surface will provide more sites to interact with DNA probes, quench the fluorescence and enhance the sensing performance. However, to the best of our knowledge, there are very few reports on using coordination polymers with a spiny surface for the sensing of nucleic acids.

Herein we report a metal–ligand coordination-driven self-assembly process for the synthesis of metal–phenolic coordination polymers with urchin-like structures and crystalline frameworks. As far as we know, this is the first report on the

The Key Laboratory of Biomedical Information Engineering of Ministry of Education, School of Life Science and Technology, Xi'an Jiaotong University Xi'an, Shaanxi 710049, P. R. China. E-mail: jingwei@xjtu.edu.cn

† Electronic supplementary information (ESI) available. See DOI: 10.1039/c8ce01555d

synthesis of urchin-like metal–phenolic coordination polymers. Due to their spiny architectures and plenty of metal species (*i.e.* Cu) and sp^2-hybridized carbon atoms on their surface, such coordination materials can be used to fabricate a fluorescence sensing platform, which can detect nucleic acid molecules in a good linear range (5–60 nM) and can even efficiently distinguish the target DNA from single-, double- and triple-base mismatched DNA.

Urchin-like MPCPs were synthesized *via* the metal–ligand coordination-driven self-assembly process (Fig. 1a). Tannic acid (TA for short) was used as a typical organic ligand. Generally, block copolymers (*i.e.* F127) and TA molecules were firstly dissolved in the alkaline water/alcohol solvents. The metal ions (*e.g.* Cu^{2+} and Zn^{2+}) were then used to crosslink TA followed by hydrothermal treatment at 100 °C for 12 hours. The metal–TA coordination crystals were obtained and denoted as Cu-TA and Zn-TA, respectively.

As the pH value can influence the coordination interactions between metal ions and catechol groups from TA, the amount of ammonia was changed to tailor the self-assembly process of metal ions and TA. In our experiments, Cu^{2+} was chosen to be a typical metal ion to form Cu-TA coordination crystals. As the amount of ammonia was increased, the coordination polymers (Cu-TA) with different structures were synthesized (Fig. 2 and S1†). The scanning electron microscopy (SEM) images showed that shuttle-like coordination polymers were obtained when the volume of ammonia was 0.4 mL. The length of the coordination polymers was around 4 μm, while the maximal diameter was around 400 nm. As the volume of ammonia was increased to 0.6 mL, the length of the shuttle-like coordination polymers decreased to 1 μm. Interestingly, such shuttle-like coordination polymers tend to aggregate together to form superstructures. When the volume of ammonia was further increased to 0.8 mL, more of the shuttle-like coordination polymers aggregated together to form the urchin-like superstructures. The diameter of the urchin-like particles was around 2.5 μm. The X-ray diffraction (XRD) patterns revealed that both the shuttle- and urchin-like coordination polymers showed crystalline frameworks, indicating the formation of the coordination crystals (Fig. 1b). As the amount of ammonia was increased, the crystalline structure remained constant.

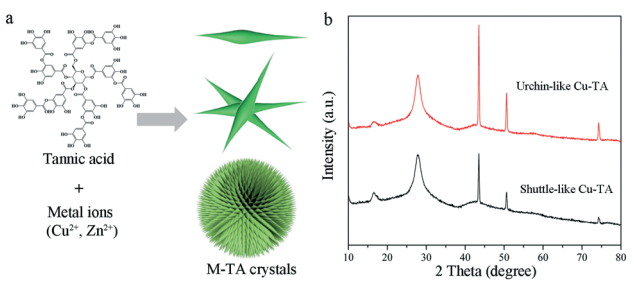

Fig. 1 (a) Schematic synthesis of metal–phenolic coordination crystals (*i.e.* M-TA). (b) XRD patterns of shuttle-like and urchin-like Cu-TA crystals.

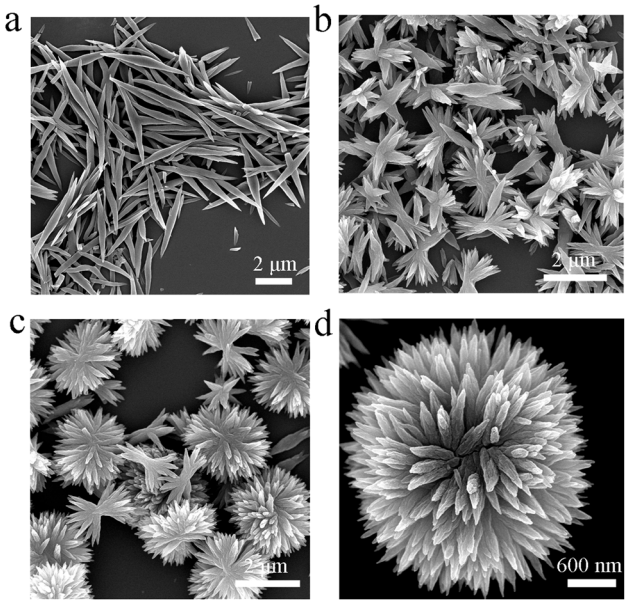

Fig. 2 SEM images of the Cu-TA crystals synthesized with different amounts of ammonia: (a) 0.4 mL, (b) 0.6 mL and (c and d) 0.8 mL.

To further demonstrate the versatility of this synthesis strategy, zinc nitrate was also used as a metal precursor. The SEM images and XRD results confirmed the formation of shuttle- and urchin-like Zn-TA coordination crystals by adjusting the amount of ammonia (Fig. S2†). Similar to the Cu-TA coordination crystals, the shuttle-like Zn-TA coordination polymers were obtained with a low amount of ammonia (*i.e.* 0.5 mL), while the urchin-like Zn-TA coordination crystals were prepared with a high content of ammonia (*i.e.* 0.8 mL). The thermogravimetry (TG) results revealed that the urchin-like Cu-TA had a larger content of metal species (22.3 wt% of Cu) than the shuttle-like Cu-TA (18.1 wt% of Cu) (Fig. S3a†). The urchin-like Zn-TA coordination polymers (22.8 wt%) also showed a higher content of Zn than the shuttle-like Zn-TA coordination polymers (19.1 wt%) (Fig. S3b†). During the synthesis process, the amount of the metal precursor remained constant. The increase of the metal contents in the coordination polymers is ascribed to the increase of ammonia in the synthesis. When the amount of ammonia was increased, more protons are dissociated from the phenolic hydroxyl groups of TA, resulting in much stronger chelating ability and more coordination sites to interact with metal ions.[2a] The X-ray photoelectron spectroscopy (XPS) spectra further confirmed the presence of metal species in the surface of the coordination crystals, which may interact with nucleic acid molecules *via* metal–ligand coordination binding (Fig. S3c and d†). The contents of C, N, O and Cu (or Zn) are shown in Fig. S3e and f.† The coordination polymers show high contents of carbon atoms (77.52 at% for Cu-TA and 74.96 at% for Zn-TA). The high-resolution C 1s spectra were fitted with three peaks at about 284.6, 285.6 and 288.4 eV, corresponding to C═C, C–C and C–O (or C═O), respectively (Fig. S4†).[7] Their relative contents were 51%, 35% and

14%, respectively. The high content of sp^2-hybridized carbon atoms would be beneficial to enhance the π–π interactions between Cu-TA and nucleic acids. Additionally, some N species were also observed due to the reaction between TA and ammonia, which is similar to our previous reports.[4g]

As the urchin-like Cu-TA coordination polymers have metal species and sp^2-hybridized carbon atoms on their surface, they would show strong interactions with nucleic acids *via* metal–ligand coordination interactions and π–π stacking. More importantly, as the Cu-TA coordination polymers with a spiny structure were used, biomolecules with large volume could be located within the coordination polymers, which can provide more interaction sites compared with the coordination polymers with a smooth surface. MicroRNAs (miRNAs) are a series of non-coding RNAs, which play important roles in human diseases like chronic lymphocytic leukemia and various cancers. Among the miRNAs, miRNA-21 is expressed at high levels in almost all solid tumors and has potential to be a biomarker for early diagnosis.[8] In this study, the DNA analogue of miRNA-21 was used as a target. The 6-carboxyfluorescein (FAM)-labeled probe DNA was designed to fabricate a MPCP-based sensing platform. As shown in Fig. 3a, the fluorescent DNA probe can be adsorbed on the urchin-like Cu-TA coordination crystals *via* metal–ligand coordination interactions and π–π stacking, resulting in fluorescence quenching.[9] When the target DNA is present, it can trigger a hybridization reaction with the probe DNA, resulting in its detachment from the Cu-TA coordination crystals and the recovery of fluorescence.

The fluorescence quenching and recovery abilities of the urchin-like Cu-TA coordination polymers were first evaluated. The FAM-labeled probe DNA (20 nM) showed strong fluorescence (Fig. 3b, black curve). After mixing with the urchin-like Cu-TA (500 μg mL^{-1}), the fluorescence intensity decreased obviously (P + Cu-TA, cyan curve). The fluorescence quenching ratio was 75.8%, indicating strong interactions between the urchin-like Cu-TA and probe DNA. When the target DNA (50 nM) was added, fluorescence were recovered with a rate of 0.892 due to the hybridization between the target and probe DNA (P + T + Cu-TA, blue curve). Note that the quenching ratio of the probe DNA/target duplex in the absence of the urchin-like Cu-TA was at 37.2% (P + T, red curve), indicating that the interaction between the urchin-like Cu-TA and dsDNA was much weaker than that between the Cu-TA and probe DNA. The formation of double-stranded structures can seal phosphate groups and nucleobases in the double helix structure, which can weaken the interactions between Cu-TA and nucleic acids. These results prove the feasibility for detecting nucleic acids using the Cu-TA based sensing platform.

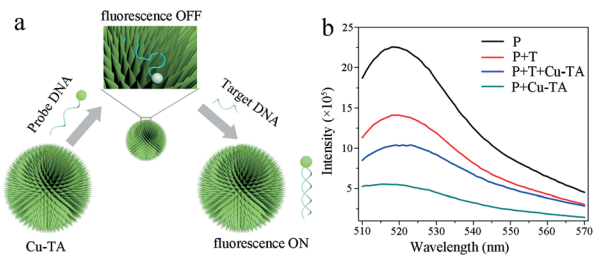

Fig. 3 (a) Schematic illustrations of the urchin-like Cu-TA crystals based on fluorescent DNA detection. (b) Fluorescence spectra of the probe DNA (P) under different conditions: P (black curve); P + target (T) (red curve); P + T + Cu-TA (blue curve); P + Cu-TA (cyan curve).

The fluorescence quenching ability of the urchin-like Cu-TA coordination polymers was further investigated (Fig. 4a). When the concentrations of Cu-TA were increased from 25 to 2000 μg mL^{-1}, the fluorescence intensity decreased gradually from 80.6 to 3.5%, suggesting a high fluorescence quenching ability of the urchin-like Cu-TA coordination crystals. The fluorescence recovery performance was then investigated by adding different amounts of the target DNA. The fluorescence increased gradually as the concentrations of the target DNA was increased from 5 to 80 nM (Fig. 4b). The fluorescence recovery efficiency (R_E) was calculated using the formula $R_E = F/F_0 - 1$, wherein F and F_0 are the fluorescence intensities at 520 nm in the presence and the absence of the target DNA, respectively. The fluorescence recovery is as high as 1.223 when the concentration of the target DNA is 80 nM. Specifically, a linear relationship between the fluorescence intensity and the concentrations of the target DNA is calculated with the concentrations ranging from 5 to 60 nM (Fig. 4c).

The specificity of the urchin-like Cu-TA coordination crystals against mismatched nucleic acid sequences is also evaluated. We used the target DNA and single-, double-, and triple-base mismatched DNA (sm-, dm- and tm-DNA) at the same concentration (*i.e.* 50 nM) to test the selectivity (Fig. 4d). Their fluorescence recovery ($F/F_0 - 1$) is 1.02, 0.38,

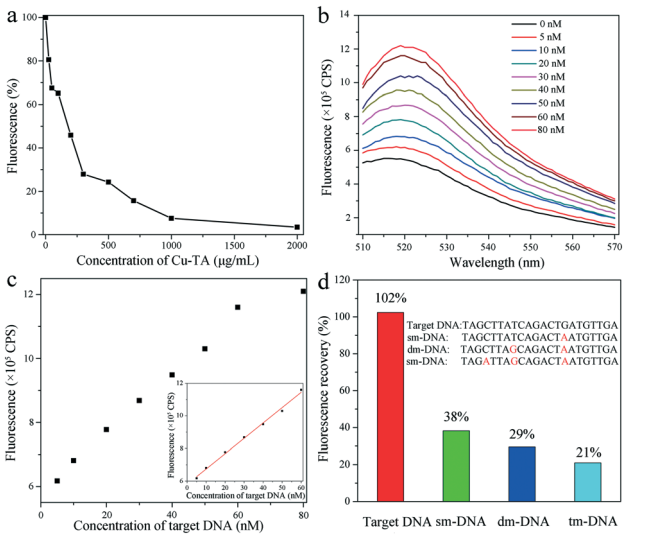

Fig. 4 (a) Fluorescence intensities of the probe DNA at 520 nm *versus* different concentrations of the urchin-like Cu-TA crystals. (b) Fluorescence recovery in different concentrations of the target DNA solution (0–80.0 nM). (c) Fluorescence intensities *versus* different concentrations of the target DNA (5–80 nM). Inset shows the corresponding calibration curve for DNA detection. (d) Selectivity for the detection of the DNA.

0.29, and 0.21, respectively. As the number of mismatched bases increases, the recovery ratio decreases, indicating the excellent selectivity of the urchin-like Cu-TA coordination crystals for the detection of nucleic acids and the ability to effectively identify single-base discrimination. The shuttle-like Cu-TA coordination polymers were also used as a sensing platform to detect nucleic acids, which also showed excellent fluorescence quenching and recovery ability (Fig. S5 and Table S1 and S2†). The sensing performance for Cu-TA coordination is comparable to that of other MOF materials (Table S3†). Such results further confirm the advantages of the Cu-TA coordination crystals when used for nucleic acid detection.

In summary, metal–phenolic coordination polymers with shuttle- and urchin-like structures and crystalline frameworks are synthesized *via* a metal–ligand coordination-driven self-assembly process. Such coordination polymers possess good fluorescence quenching and recovery abilities and can be used as a highly efficient, sensitive and selective fluorescent sensor for nucleic acid detection. The urchin-like metal–phenolic coordination polymers are further used to detect the DNA analogue of miRNA-21 with high sensitivity. This sensing platform can even efficiently distinguish the target DNA from single-, double- and triple-base mismatched DNA. It is believed that the synthesis of coordination polymers with intricate structures will provide more possibilities to tailor their physiochemical properties and extend their applications in sensors, biomedicine and energy science.

This work was financially supported by the National Science Foundation of China (No. 21701130), the Fundamental Research Funds for the Central Universities and the "Young Talent Support Plan" of Xi'an Jiaotong University. We thank Mr. Zijun Ren at the Instrument Analysis Center of Xi'an Jiaotong University for his assistance with the SEM analysis.

Conflicts of interest

There are no conflicts to declare.

Notes and references

1 (*a*) H. Li, M. Eddaoudi, M. O'Keeffe and O. M. Yaghi, *Nature*, 1999, **402**, 276–279; (*b*) J. S. Seo, D. Whang, H. Lee, S. I. Jun, J. Oh, Y. J. Jeon and K. Kim, *Nature*, 2000, **404**, 982–986; (*c*) S. Kitagawa, R. Kitaura and S. Noro, *Angew. Chem., Int. Ed.*, 2004, **43**, 2334–2375; (*d*) J. Lee, O. K. Farha, J. Roberts, K. A. Scheidt, S. T. Nguyen and J. T. Hupp, *Chem. Soc. Rev.*, 2009, **38**, 1450–1459; (*e*) J. R. Li, R. J. Kuppler and H. C. Zhou, *Chem. Soc. Rev.*, 2009, **38**, 1477–1504; (*f*) L. E. Kreno, K. Leong, O. K. Farha, M. Allendorf, R. P. Van Duyne and J. T. Hupp, *Chem. Rev.*, 2012, **112**, 1105–1125; (*g*) Z. Hu, B. J. Deibert and J. Li, *Chem. Soc. Rev.*, 2014, **43**, 5815–5840; (*h*) Q.-L. Zhu and Q. Xu, *Chem. Soc. Rev.*, 2014, **43**, 5468–5512; (*i*) T. Rodenas, I. Luz, G. Prieto, B. Seoane, H. Miro, A. Corma, F. Kapteijn, F. X. Llabres i Xamena and J. Gascon, *Nat. Mater.*, 2015, **14**, 48–55; (*j*) Y. Cui, B. Li, H. He, W. Zhou, B. Chen and G. Qian, *Acc. Chem. Res.*, 2016, **49**, 483–493; (*k*) E. Gkaniatsou, C. Sicard, R. Ricoux, J. P. Mahy, N. Steunou and C. Serre, *Mater. Horiz.*, 2017, **4**, 55–63; (*l*) W. P. Lustig, S. Mukherjee, N. D. Rudd, A. V. Desai, J. Li and S. K. Ghosh, *Chem. Soc. Rev.*, 2017, **46**, 3242–3285; (*m*) I. Stassen, N. Burtch, A. Talin, P. Falcaro, M. Allendorf and R. Ameloot, *Chem. Soc. Rev.*, 2017, **46**, 3185–3241; (*n*) B. Yan, *Acc. Chem. Res.*, 2017, **50**, 2789–2798; (*o*) Y. Zhang, S. Yuan, G. Day, X. Wang, X. Yang and H. C. Zhou, *Coord. Chem. Rev.*, 2018, **354**, 28–45; (*p*) X. Fang, L. Hu, C. Ye and L. Zhang, *Pure Appl. Chem.*, 2010, **82**, 2185–2198; (*q*) P. Yu, K. Hu, H. Chen, L. Zheng and X. Fang, *Adv. Funct. Mater.*, 2017, **27**, 1703166.

2 (*a*) H. Ejima, J. J. Richardson, K. Liang, J. P. Best, M. P. van Koeverden, G. K. Such, J. Cui and F. Caruso, *Science*, 2013, **341**, 154–157; (*b*) J. Wei, Y. Liang, Y. Hu, B. Kong, J. Zhang, Q. Gu, Y. Tong, X. Wang, S. P. Jiang and H. Wang, *Angew. Chem., Int. Ed.*, 2016, **55**, 12470–12474; (*c*) H. Ejima, J. J. Richardson and F. Caruso, *Nano Today*, 2017, **12**, 136–148.

3 A. Sanchez-Sanchez, M. Teresa Izquierdo, S. Mathieu, J. Gonzalez-Alvarez, A. Celzard and V. Fierro, *Green Chem.*, 2017, **19**, 2653–2665.

4 (*a*) J. Guo, Y. Ping, H. Ejima, K. Alt, M. Meissner, J. J. Richardson, Y. Yan, K. Peter, D. von Elverfeldt, C. E. Hagemeyer and F. Caruso, *Angew. Chem., Int. Ed.*, 2014, **53**, 5546–5551; (*b*) F. Liu, X. He, H. Chen, J. Zhang, H. Zhang and Z. Wang, *Nat. Commun.*, 2015, **6**, 8003; (*c*) J. Guo, B. L. Tardy, A. J. Christofferson, Y. Dai, J. J. Richardson, W. Zhu, M. Hu, Y. Ju, J. Cui, R. R. Dagastine, I. Yarovsky and F. Caruso, *Nat. Nanotechnol.*, 2016, **11**, 1105–1111; (*d*) J. Wei, Y. Liang, Y. Hu, B. Kong, G. P. Simon, J. Zhang, S. P. Jiang and H. Wang, *Angew. Chem., Int. Ed.*, 2016, **55**, 1355–1359; (*e*) B. J. Kim, S. Han, K.-B. Lee and I. S. Choi, *Adv. Mater.*, 2017, **29**, 1700784; (*f*) P. Zhang, L. Wang, S. Yang, J. A. Schott, X. Liu, S. M. Mahurin, C. Huang, Y. Zhang, P. F. Fulvio, M. F. Chisholm and S. Dai, *Nat. Commun.*, 2017, **8**, 15020; (*g*) J. Wei, G. Wang, F. Chen, M. Bai, Y. Liang, H. Wang, D. Zhao and Y. Zhao, *Angew. Chem., Int. Ed.*, 2018, **57**, 9838–9843.

5 (*a*) L. Chen, H. Zheng, X. Zhu, Z. Lin, L. Guo, B. Qiu, G. Chen and Z. N. Chen, *Analyst*, 2013, **138**, 3490–3493; (*b*) X. Zhu, H. Zheng, X. Wei, Z. Lin, L. Guo, B. Qiu and G. Chen, *Chem. Commun.*, 2013, **49**, 1276–1278; (*c*) J. M. Fang, F. Leng, X. J. Zhao, X. L. Hu and Y. F. Li, *Analyst*, 2014, **139**, 801–806; (*d*) H. T. Zhang, J. W. Zhang, G. Huang, Z. Y. Du and H. L. Jiang, *Chem. Commun.*, 2014, **50**, 12069–12072; (*e*) J. Tian, Q. Liu, J. Shi, J. Hu, A. M. Asiri, X. Sun and Y. He, *Biosens. Bioelectron.*, 2015, **71**, 1–6; (*f*) L. Qin, L. X. Lin, Z. P. Fang, S. P. Yang, G. H. Qiu, J. X. Chen and W. H. Chen, *Chem. Commun.*, 2016, **52**, 132–135; (*g*) Y. Peng, Y. Huang, Y. Zhu, B. Chen, L. Wang, Z. Lai, Z. Zhang, M. Zhao, C. Tan, N. Yang, F. Shao, Y. Han and H. Zhang, *J. Am. Chem. Soc.*, 2017, **139**, 8698–8704; (*h*) H. S. Wang, *Acc. Chem. Res.*, 2017, **349**, 139–155; (*i*) H. S. Wang, H. L. Liu, K. Wang, Y. Ding, J. J. Xu, X. H. Xia and H. Y. Chen, *Anal. Chem.*,

2017, **89**, 11366–11371; (*j*) Z. Wang, Y. Fu, Z. Kang, X. Liu, N. Chen, Q. Wang, Y. Tu, L. Wang, S. Song, D. Ling, H. Song, X. Kong and C. Fan, *J. Am. Chem. Soc.*, 2017, **139**, 15784–15791; (*k*) L. Esfandiari, H. G. Monbouquette and J. J. Schmidt, *J. Am. Chem. Soc.*, 2012, **134**, 15880–15886.

6 (*a*) H. Song, M. Yu, Y. Lu, Z. Gu, Y. Yang, M. Zhang, J. Fu and C. Yu, *J. Am. Chem. Soc.*, 2017, **139**, 18247–18254; (*b*) D. G. Montjoy, J. H. Bahng, A. Eskafi, H. Hou and N. A. Kotov, *J. Am. Chem. Soc.*, 2018, **140**, 7835–7845; (*c*) L. B. Gulina, V. P. Tolstoy, I. A. Kasatkin and I. V. Murin, *CrystEngComm*, 2017, **19**, 5412.

7 T. I. T. Okpalugo, P. Papakonstantinou, H. Murphy, J. McLaughlin and N. M. D. Brown, *Carbon*, 2005, **43**, 153–161.

8 (*a*) L. B. Frankel, N. R. Christoffersen, A. Jacobsen, M. Lindow, A. Krogh and A. H. Lund, *J. Biol. Chem.*, 2008, **283**, 1026–1033; (*b*) Z. Lu, M. Liu, V. Stribinskis, C. M. Klinge, K. S. Ramos, N. H. Colburn and Y. Li, *Oncogene*, 2008, **27**, 4373–4379; (*c*) T. Thum, C. Gross, J. Fiedler, T. Fischer, S. Kissler, M. Bussen, P. Galuppo, S. Just, W. Rottbauer, S. Frantz, M. Castoldi, J. Soutschek, V. Koteliansky, A. Rosenwald, M. A. Basson, J. D. Licht, J. T. R. Pena, S. H. Rouhanifard, M. U. Muckenthaler, T. Tuschl, G. R. Martin, J. Bauersachs and S. Engelhardt, *Nature*, 2008, **456**, 980–983; (*d*) R. Rupaimoole, G. A. Calin, G. Lopez–Berestein and A. K. Sood, *Cancer Discovery*, 2016, **6**, 235–246.

9 (*a*) B. Liu and J. Liu, *ACS Appl. Mater. Interfaces*, 2015, **7**, 24833–24838; (*b*) C. Lu, Z. Huang, B. Liu, Y. Liu, Y. Ying and J. Liu, *Angew. Chem., Int. Ed.*, 2017, **56**, 6208–6212; (*c*) S. He, B. Song, D. Li, C. Zhu, W. Qi, Y. Wen, L. Wang, S. Song, H. Fang and C. Fan, *Angew. Chem., Int. Ed.*, 2010, **20**, 453–459; (*d*) H. Zhang, H. Zhang, A. Aldalbahi, X. Zuo, C. Fan and X. Mi, *Biosens. Bioelectron.*, 2017, **89**, 96–106.

